



Research Article

## An application of conventional and advanced exergy approaches on a R41/R1233ZD(E) cascade refrigeration system under optimum conditions

Center AKTEMUR<sup>1,\*</sup>, Servet Giray HACIPASAOGLU<sup>1</sup>

<sup>1</sup>Department of Mechanical Engineering, Kocaeli University, Umuttepe Campus, 41380 Kocaeli, Turkey

### ARTICLE INFO

#### Article history

Received: 20 November 2020

Accepted: 22 January 2021

#### Keywords:

Cascade Refrigeration System,  
Advanced Exergy Analysis,  
Conventional Exergy Analysis;  
R41, R1233zd(E)

### ABSTRACT

Painstaking adjustment of an optimum low-temperature cycle (LTC) condenser temperature allows cascade refrigeration system (CRS) to operate at maximum performance. This study exhibits an original approach because, for the first time, advanced exergy analysis is implemented under an optimum LTC condenser temperature of CRS operating with R41/R1233zd(E) as an environmentally-friendly refrigerant pair. Under the auspices of advanced exergy analysis, there is endogenous exergy destruction of 50.43% and exogenous exergy destruction of 49.57% within total exergy destruction. It is pointed out that the interactions between the CRS components (external irreversibilities) are partly less than exergy destruction that occurs within components (internal irreversibilities). The avoidable part within total exergy destruction, which is greater than the unavoidable part, indicates that components have a high improvement potential with a value of 56.31%. Furthermore, LTC compressor depends significantly on other components, as it has the largest exogenous part of exergy destruction with 75.82%. The results indicate that the CRS's exergy efficiency, which can be determined based on conventional exergy analysis, is only 36%. However, this increases to 68% with the improvements needed for the components.

**Cite this article as:** Center A, Servet G H. An application of conventional and advanced exergy approaches on a R41/R1233ZD(E) cascade refrigeration system under optimum conditions. J Ther Eng 2022;8(2):182–201.

### INTRODUCTION

Refrigeration is a prerequisite for human comfort, peace and health, and it is also vital to industrial processes, electronic devices and applications in food preservation [1]. Refrigeration systems are increasingly demanding more energy, a situation that introduces numerous ecological

challenges, such as global warming [2]. The use of refrigerants with high Global Warming Potential (GWP) and Ozone Depletion Potential (ODP), which contribute cardinally to global warming and thereby affect people's health,

\*Corresponding author.

\*E-mail address: [cenkeraktemur41@gmail.com](mailto:cenkeraktemur41@gmail.com)

This paper was recommended for publication in revised form by Regional Editor Ozgen Acikgoz



has become an attention-grabbing issue. Some restrictions and prohibitions on the use of refrigerants have been introduced through decisions made due to international agreements and policies, such as the F-gas Regulation, the Kyoto Protocol, the Montreal Protocol and the Paris Agreement [3]. Chlorofluorocarbons (CFCs), a part of the most common first-generation refrigerant group and among the substances that destroy the ozone layer, were the first prohibited refrigerants [4,5]. Hydrochlorofluorocarbons (HCFCs), which are identified as second-generation refrigerants, have a wide range of uses. Still, since they contain chlorine atoms (as do the CFCs), they destroy the stratospheric ozone due to a high GWP and an ODP higher than zero [6]. It is intended to completely ban the use, production and import of all the refrigerants in this class by 2030 [7]. Hydrofluorocarbons (HFCs), which are categorised as third-generation refrigerants and cause less environmental anxiety than the previous generations of refrigerants, currently have an extensive range of utilisation. Nevertheless, the Kigali amendment to the Montreal Protocol has led to the gradual reduction of traditional HFC refrigerants with high GWP [8]. Hydrofluoro-olefins (HFOs), which have emerged as the fourth- or next-generation refrigerants, have very low GWP and zero ODP values and therefore have little or no undesirable impact on the environment [9,10]. With these considerations in mind, new studies are examining refrigerants in the HFO-class to promote environmental sustainability [11-15].

Five different approaches in reliance on the application of advanced exergy analysis have been reported by Ref. [16]. These five approaches include: (1) the engineering method, (2) the thermodynamic cycle method, (3) the structural theory method, (4) the exergy balance method and (5) the equivalent components method. The thermodynamic cycle method for advanced exergy analysis is the most convenient and produces the best results for different cases (ideal, real and unavoidable) where a thermodynamic cycle can be defined [17]. Despite numerous papers considering the advantages of conventional exergy analysis, the mutual interdependencies present in the system components are beyond the scope of conventional exergy analysis; such methods are unable to evaluate the real potential for improving the components. In the thermodynamic cycle method for advanced exergy analysis, it is possible to do this because the destruction of each component's exergy is split into avoidable/unavoidable and endogenous/exogenous parts [18]. Such splitting approaches enable the designer and operator of an energy conversion system to identify efficiency optimisation strategies. Not only is the accuracy of exergy analysis promoted by this splitting, but this method also enhances the understanding of how thermodynamic inefficiencies occur, as well as offering opportunities to analyse exergy-based performance concerning exergo-economic and exergo-environmental factors [19, 20].

Looking deeply into the open literature, the adoption of advanced exergy approach, particularly in the analysis of ejector -based refrigeration systems and absorption refrigeration systems, has attracted a great deal of attention. A summary of the studies carried out in the field of refrigeration is given in Table 1.

Closely reviewing the literature finds that a vast number of studies examine the conventional exergy-based thermodynamic analysis of cascade refrigeration systems (CRSs) using various refrigerant pairs such as R41-R404A and R41-R161 [21], R744-R717 [22], R744-R134A [23], R404A-R134A [24], N<sub>2</sub>O-R744 [25], R744-HFE7000 [26], R41-R404A and R23-R404A [27], R410A-R23 and R404A-R508B [28], R134A- R410A [29], R134A-R744 and R152A-R744 [30], R744-R717, R744-R290, R744-R1270, R744-R404A and R744-R12 [31], R744-R717, R744-R290, R744-R600, R744-R404A, R744-R410A and R744-R134 [32], 56 possible combinations of refrigerant pairs [33] and R170-R161 and R41-R404A [34].

In this study, R41, which is considered appropriate for use at low temperatures and recommended, is used. R1233zd (E), which is one of the new generation refrigerants, is recommended for HTC. This refrigerant has no explosive and flammable properties. Thus, the combination of R41/R1233zd(E) is proposed to perform advanced exergy analysis of the CRS. There is only one study in the literature on advanced exergy analysis of the CRS conducted by Gholamian et al. [35]. They used R744 in the low-temperature cycle (LTC) and R717 in the high-temperature cycle (HTC). However, they did not care about optimum LTC temperatures. Determining a LTC condenser temperature, which is a crucial indicator for achieving the best performance from the standpoint of energy- and exergy-based parameters is necessary because it plays a pivotal role in the operation of the CRSs. This study is the first which focuses on finding an optimum LTC condenser temperature for ideal, real and unavoidable thermodynamic cycles before splitting the exergy destruction into avoidable/unavoidable and endogenous/exogenous parts of the CRS. The main aim of using the advanced exergy approach by splitting exergy destruction into various parts is to procure more detailed knowledge regarding the levels of interaction (endogenous/exogenous) among the components, to identify the improving potential of the system (avoidable/unavoidable), and to give conceivable suggestions aimed at enhancing the system efficiency.

## CYCLE DESCRIPTION

The CRS is a refrigeration system that is widely used in applications where low temperature is required, consisting of two vapour-compression refrigeration systems connected with a cascade heat exchanger or cascade condenser, where R41 (fluoromethane) [53] is used in LTC for cooling, and R1233zd(E) (trans-1-Chloro-3,3,3-trifluoropropene) [54]

**Table 1.** The previous studies based on advanced exergy in the field of refrigeration

Author	System	Refrigerant	Remarks
Ustaoglu [18]	Compression-absorption cascade refrigeration	R134a, R152a, R717, R290, R502, R507a in vapor-compression NH <sub>3</sub> /H <sub>2</sub> O in absorption	The most significant potential for improvement is associated with the generator.
Morosuk et al. [36]	Two-stage refrigeration	R717	Exergy destruction in the condenser can fall significantly due to evaporator improvement.
Yu et al. [37]	Cascade absorption refrigeration	NH <sub>3</sub> /H <sub>2</sub> O LiBr/H <sub>2</sub> O	The endogenous part of almost all exergy destruction rates and the attendant exergy destruction cost rates have been documented.
Aman et al. [38]	Absorption air conditioning	LiCl/H <sub>2</sub> O	57% of total exergy destruction is avoidable, whereas 43% is unavoidable.
Ustaoglu et al. [39]	Ejector refrigeration	R290, R141b, R142b, R134A, R152A, R600A	For R600a, the generator is associated with tremendous potential for improvement.
Gholamian et al. [35]	Cascade refrigeration	R744/R717	System efficiency can increase by approximately 42.13% due to component improvement.
Zhao et al. [40]	Parallel and series compression-ejection hybrid refrigeration	R290	The compressor improved by 41.28% for the series system, but the most significant improvement was associated with the parallel system.
Sarkar and Joshi [41]	Subcritical and transcritical refrigeration	R744, R717, R404a.	The most potential for improvement was associated with the compressor, while it was evaporator for R717.
Colorado-Garrido [42]	Compression-absorption cascade refrigeration	R134A in vapour-compression LiBr/H <sub>2</sub> O in absorption	The evaporator was associated with the greatest potential for improvement.
Gong and Boulama [43]	Absorption refrigeration	LiBr/H <sub>2</sub> O	The exogenous and avoidable parts of exergy destruction of the absorber are higher than that of the generator.
Morosuk and Tsatsaronis [20]	Vapor-compression refrigeration	R125, R134A, R22, R717, R500, R407C	Increasing the system's thermodynamic performance can be achieved by improving the first evaporator and then the compressor.
Bai et al. [46]	Ejector expansion transcritical refrigeration	R744	The dominantly endogenous part of the system's exergy destruction should be recognised, and it is possible to improve the system components to avoid 43.44% of total exergy destruction.
Chen et al. [47]	Ejector refrigeration	R245fa	Ejector, generator and condenser should be taken into consideration to increase the performance of the overall system.
Morosuk and Tsatsaronis [48]	Vapor-compression refrigeration Simple gas-turbine power cycle	R717 in refrigeration cycle CH <sub>4</sub> in gas-turbine cycle	There are essential differences in the exergy destruction rates of the endogenous part.
Modi et al. [49]	Vapor-compression refrigeration	R134a, R143m, R1234yf, R161, R513A, R1270	Endogenous-avoidable part of the exergy destruction for the evaporator is 26.38%.
Gullo et al. [50]	Booster refrigeration system with parallel compression	R744	Improving gas cooler/condenser could be achieved by reducing inefficiencies of medium temperature evaporator.
Liu [51]	Booster-assisted ejector refrigeration	R600A	As a result of the component efficiency improvement, 55.5% of the total exergy destruction can be avoided.
Bai et al. [52]	Modified auto-cascade freezer cycle with an ejector	Mixing of R134A/R23 (0.5/0.5)	Increased compressor and ejector efficiencies can dramatically bring down the unavoidable endogenous part of the exergy destruction.

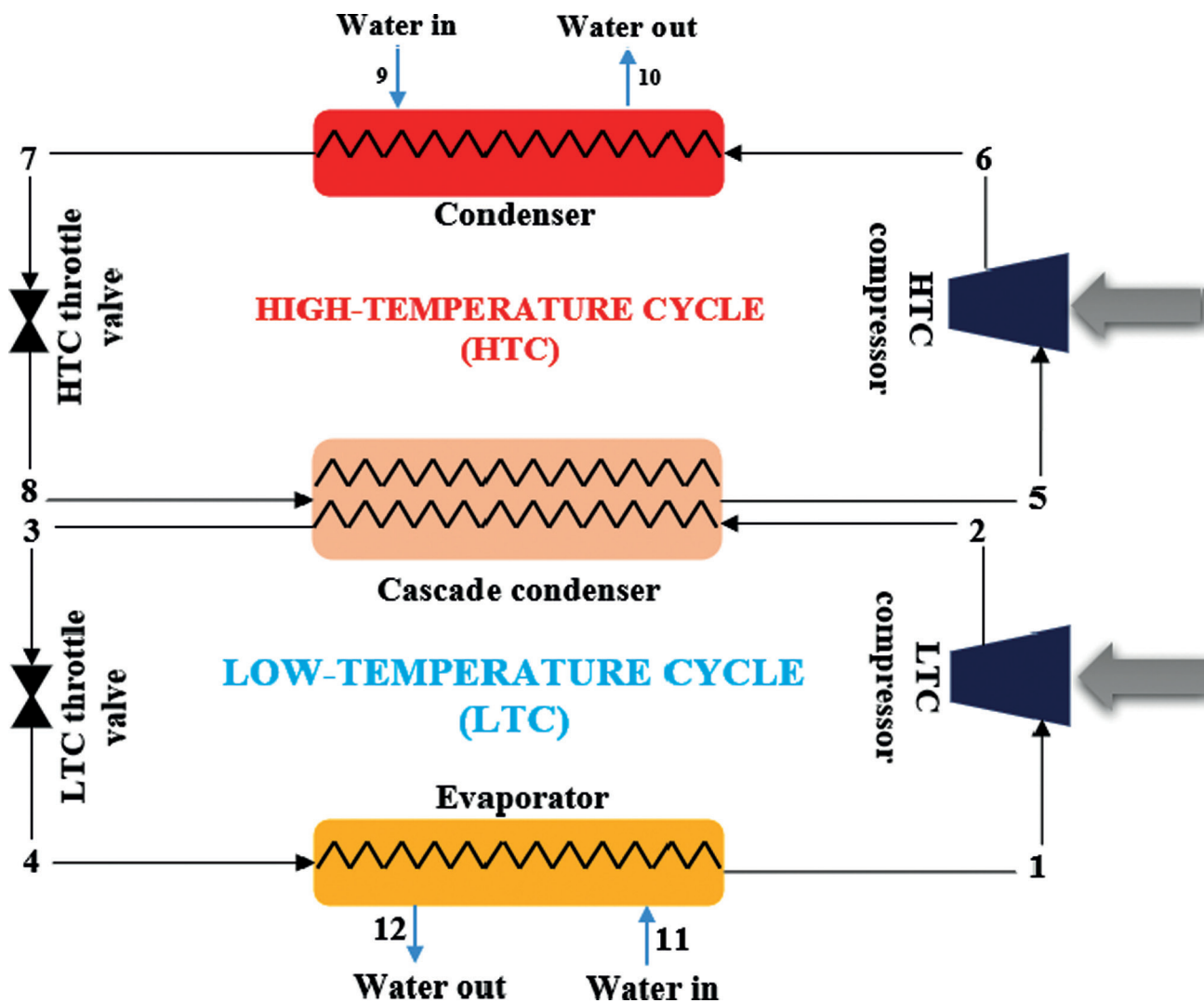


Figure 1. A schematic representation of the CRS.

Table 2. Thermophysical, environmental and safety properties of the recommended refrigerants

Cycle	Refrigerant	Class	Thermodynamic data				Environmental data			Safety data	
			M (kg/kmol)	$T_{cr}$ (°C)	$P_{cr}$ (MPa)	NBP (°C)	ODP	GWP (100-year)	ALT (year)	LFL (%)	Safety class
LTC	R41	HFC	34	44.1	5.9	-78.1	0	97	2.4	6.8	A2
HTC	R1233zd(E)	HFO	130.5	154	3.57	18	0	7	0.01	None	A1

M,  $T_{cr}$ ,  $P_{cr}$ , NBP, ALT, LFL stand for molecular weight, critical temperature, critical pressure, normal boiling point, atmospheric lifetime, lower flammable limit, respectively.

is utilised in the high-temperature cycle (HTC) to condense the refrigerant circulating in LTC. The working principle of the CRSs is the same with single-stage vapour compression refrigeration systems except for one difference. This difference is the cascade heat exchanger, a compact component

that acts as an evaporator in LTC and a condenser in HTC. It is assumed that the cascade heat exchanger is well-insulated [55]; therefore, the heat delivered by the R41 in LTC is equal to the heat received by the R1233zd(E) in HTC. A schematic diagram represented by the subcritical CRS

is depicted in Figure 1. The thermo-physical, environmental and safety properties of the refrigerants, as mentioned above, are listed in Table 2 [12,27,34,56].

### ASSUMPTIONS MADE IN THE ANALYSIS

The analysis of the CRS can be simplified based on suppositions found in the literature [14, 21, 27, 34, 35]. These simplifications are as follows:

- Heat losses and pressure drops in connection pipes and system components are not taken into account.
- All components of the CRS are considered to be a steady-state and steady-flow process.
- Both the compression and expansion processes are adiabatic.
- Electricity consumptions of condenser and evaporator fans are disregarded.
- The condenser and CHX have outlet state of the saturated liquid phase, while the evaporator has outlet state of the saturated vapour phase.
- The refrigeration load of the subcritical CRS is 1 kW.
- The CRS utilises liquid water as the brine side fluids for condenser and evaporator. The inlet and the outlet temperatures of water are kept at:  $T_9 = 25^\circ\text{C}$ ,  $T_{10} = 30^\circ\text{C}$ ,  $T_{11} = -50^\circ\text{C}$ ,  $T_{12} = -55^\circ\text{C}$ .

**Table 3.** Default values of the real cycle for thermodynamic assessment

Parameter	Input
Evaporator temperature, $T_{ev}$	$-60^\circ\text{C}$
Condenser temperature, $T_{cond}$	$40^\circ\text{C}$
Isentropic efficiencies of LTC and HTC compressors, $\eta_i$	$1 - (0.04 \times P_r)$
The temperature difference in CHX, $\Delta T$	$5^\circ\text{C}$

$P_r$  refers to compressor compression ratios in LTC and HTC.

- The reference state (dead state) is the ambient temperature ( $T_0$ ) of  $25^\circ\text{C}$  and pressure ( $P_0$ ) of  $101.325$  kPa.

### DETERMINATION OF THE CRS PARAMETERS

Advanced exergy analysis requires assumptions for real, ideal and unavoidable cycles. The operating parameters of the real cycle are given in Table 3 [12,34–36]. Table 4 presents the real, ideal and unavoidable conditions for each CRS component, as suggested by Ref. [35, 61]. The real and unavoidable conditions are used to find the avoidable/unavoidable parts in the advanced exergy analysis. The real and ideal conditions are used to find the endogenous/exogenous parts. The unavoidable cycle conditions are between real and ideal conditions.

### METHODOLOGY

Conventional and advanced exergy analyses are undertaken to assess the CRS under an optimum LTC condenser temperature for thermodynamic analysis. The equations used for these computations are presented in the following sub-sections.

### ENERGY TERMS

The input and output conditions underpinning many engineering systems' operation stay unchanged for lengthy intervals. This is exemplified by the elements of a refrigeration system (e.g. condenser, evaporator, throttle valve, compressor), which are operational for extensive periods before system maintenance. For this reason, such systems are examined as steady-flow processes. The mass and the overall energy of the control volume do not fluctuate in these open systems [57]. The conservation of mass and energy conservation for continuous-flow open systems are established by Eqs. (1) and (2), respectively. For the CRS

**Table 4.** Main data required for the CRS to operate in the real, ideal and unavoidable circumstances

Component	Real	Theoretical	Unavoidable
LTC compressor	$\eta_i = 1 - (0.04 \times P_{r,LTC})$	$\eta_i = 1$	$\eta_i = 1 - (0.04 \times P_r)$
HTC compressor	$\eta_i = 1 - (0.04 \times P_{r,HTC})$	$\eta_i = 1$	$\eta_i = 1 - (0.04 \times P_r)$
Evaporator	$\Delta T_{ev}^{RL} = 5^\circ\text{C}$	$\Delta T_{ev}^{TH} = 0^\circ\text{C}$	$\Delta T_{ev}^{UN} = 3^\circ\text{C}$
Condenser	$\Delta T_{cond}^{RL} = 10^\circ\text{C}$	$\Delta T_{cond}^{TH} = 0^\circ\text{C}$	$\Delta T_{cond}^{UN} = 5^\circ\text{C}$
LTC throttle valve	Isenthalpic process ( $h_3 = h_4$ )	Isentropic process <sup>a</sup> ( $s_3 = s_4$ )	Isenthalpic process ( $h_3 = h_4$ )
HTC throttle valve	Isenthalpic process ( $h_7 = h_8$ )	Isentropic process <sup>a</sup> ( $s_7 = s_8$ )	Isenthalpic process ( $h_7 = h_8$ )
Cascade condenser	$\Delta T_{CHX}^{RL} = 5^\circ\text{C}$	$\Delta T_{CHX}^{TH} = 0^\circ\text{C}$	$\Delta T_{CHX}^{UN} = 3^\circ\text{C}$

<sup>a</sup>A throttling process is always irreversible for real and unavoidable cycles; consequently, a throttling valve is assumed to be replaced by an isentropic expander for an ideal cycle [17,18,20].

**Table 5.** Energy and mass balance relations

Component	Mass balance	Energy balance
Evaporator	$\dot{m}_{LTC} = \dot{m}_1 = \dot{m}_4$ $\dot{m}_{w,ev} = \dot{m}_{11} = \dot{m}_{12}$	$\dot{Q}_{ev} = \dot{m}_{LTC}(h_1 - h_4)$ $\dot{m}_{LTC}(h_1 - h_4) = \dot{m}_{w,ev}(h_{11} - h_{12})$
LTC compressor	$\dot{m}_{LTC} = \dot{m}_1 = \dot{m}_2$	$\dot{W}_{LTC} = \frac{\dot{m}_{LTC}(h_{2s} - h_1)}{\eta_i}$
LTC throttle valve	$\dot{m}_{LTC} = \dot{m}_3 = \dot{m}_4$	$h_3 = h_4$
Cascade condenser	$\dot{m}_{LTC} = \dot{m}_2 = \dot{m}_3$ $\dot{m}_{HTC} = \dot{m}_5 = \dot{m}_8$	$\dot{Q}_{CC} = \dot{m}_{LTC}(h_2 - h_3) = \dot{m}_{HTC}(h_5 - h_8)$
Condenser	$\dot{m}_{HTC} = \dot{m}_6 = \dot{m}_7$ $\dot{m}_{w,cond} = \dot{m}_9 = \dot{m}_{10}$	$\dot{Q}_{cond} = \dot{m}_{HTC}(h_6 - h_7)$ $\dot{m}_{HTC}(h_6 - h_7) = \dot{m}_{w,cond}(h_{10} - h_9)$
HTC compressor	$\dot{m}_{HTC} = \dot{m}_6 = \dot{m}_5$	$\dot{W}_{HTC} = \frac{\dot{m}_{HTC}(h_{6s} - h_5)}{\eta_i}$
HTC throttle valve	$\dot{m}_{HTC} = \dot{m}_7 = \dot{m}_8$	$h_7 - h_8$
Overall system	$COP = \frac{\dot{Q}_{ev}}{\dot{W}_{LTC} + \dot{W}_{HTC}}$	

and its components, the mass and energy balance equations are also illustrated in Table 5 [58].

$$\sum_{in} \dot{m} = \sum_{out} \dot{m} \tag{1}$$

$$\dot{Q} - \dot{W} + \sum_{in} \dot{m}h - \sum_{out} \dot{m}h = 0 \tag{2}$$

**EXERGY TERMS**

The term exergy denotes the potential that an available amount of energy can be converted into work [59]. The computation of this potential depends on environmental and energy conditions and is an expression of the highest amount of work that can be obtained. The lost work potential during a process change is defined as irreversibility or exergy destruction. The less the exergy destruction during a process change, the more the work produced or, the less the work consumed [60]. Analysis of conventional exergy denotes a thermodynamic analysis whose foundation is the second law, facilitating a significant and realistic assessment and comparison of state changes and energy systems. Exergy balance for any control volume at steady state is obtained by Eq. (3) [61].

$$\sum \left( 1 - \frac{T_0}{T} \right) \dot{Q} - \dot{W} + \sum_{(in)}^F m e_F - \sum_{(out)}^P m e_P - \dot{E}_D = 0 \tag{3}$$

The total exergy of a system without magnetic, electrical, nuclear and surface tension effects is expressed by  $\dot{E}$ . Exergy is divided into four groups as chemical exergy  $\dot{E}^{CH}$ , physical exergy  $\dot{E}^{PH}$ , kinetic exergy  $\dot{E}^{KE}$  and potential exergy  $\dot{E}^{PE}$ , as indicated in Eq. (4) [61]. The total exergy of the refrigerant flow for the unit mass can be obtained by Eq. (5) [61]. In this study, chemical exergy has a null value in the present work because the modelled CRS system is free of a chemical reaction. The assumption is that there are insignificant changes in the system kinetic and potential exergy. Consequently, Eq. (6) [35] helps to determine the flow of physical exergy associated with the unit mass. The exergy balance equations of components of the CRS are also illustrated in Table 6 [34, 58], while the other performance parameters are found by Eqs. (4)-(6) [17,19,36,39,40,47,62].

$$\dot{E} = \dot{E}^{CH} + \dot{E}^{PH} + \dot{E}^{KE} + \dot{E}^{PE} \tag{4}$$

$$e = e^{CH} + e^{PH} + e^{KE} + e^{PE} \tag{5}$$

$$e^{PH} = h - h_0 - T_0(s - s_0) \tag{6}$$

The conventional exergy efficiency of the overall system is obtained by Eq. (7).

$$\epsilon_{tot} = \frac{\dot{E}_{P,tot}}{\dot{E}_{F,tot}} \tag{7}$$

**Table 6.** Conventional exergy balance equations

Component	Exergy of fuel (or driving input) ( $\dot{E}_{F,k}$ )	Exergy of the product (or desired value) ( $\dot{E}_{P,k}$ )	Exergy destruction (or internal exergy loss) ( $\dot{E}_{D,k}$ )
Evaporator	$\dot{E}_{F,ev} = \dot{m}_L(e_4 - e_1)$	$\dot{E}_{P,ev} = \dot{m}_{w,ev}(e_{12} - e_{11})$	$\dot{E}_{D,ev} = \dot{E}_{F,ev} - \dot{E}_{P,ev}$
LTC compressor	$\dot{E}_{F,LTC\ comp} = \dot{W}_{LTC}$	$\dot{E}_{P,LTC\ comp} = \dot{m}_L(e_2 - e_1)$	$\dot{E}_{D,LTC\ comp} = \dot{E}_{F,LTC\ comp} - \dot{E}_{P,LTC\ comp}$
LTC throttle valve	$\dot{E}_{F,LTC\ tv} = \dot{m}_L e_3$	$\dot{E}_{P,LTC\ tv} = \dot{m}_L e_4$	$\dot{E}_{D,LTC\ tv} = \dot{E}_{F,LTC\ tv} - \dot{E}_{P,LTC\ tv}$
Cascade condenser	$\dot{E}_{F,CHX} = \dot{m}_L(e_2 - e_5)$	$\dot{E}_{P,CHX} = \dot{m}_L(e_3 - e_8)$	$\dot{E}_{D,CHX} = \dot{E}_{F,CHX} - \dot{E}_{P,CHX}$
Condenser	$\dot{E}_{F,cond} = \dot{m}_H(e_6 - e_7)$	$\dot{E}_{P,cond} = \dot{m}_{w,cond}(e_{10} - e_9)$	$\dot{E}_{D,cond} = \dot{E}_{F,cond} - \dot{E}_{P,cond}$
HTC compressor	$\dot{E}_{F,HTC\ comp} = \dot{W}_{HTC}$	$\dot{E}_{P,HTC\ comp} = \dot{m}_H(e_6 - e_5)$	$\dot{E}_{D,HTC\ comp} = \dot{E}_{F,HTC\ comp} - \dot{E}_{P,HTC\ comp}$
HTC throttle valve	$\dot{E}_{F,HTC\ tv} = \dot{m}_H e_7$	$\dot{E}_{P,HTC\ tv} = \dot{m}_H e_8$	$\dot{E}_{D,HTC\ tv} = \dot{E}_{F,HTC\ tv} - \dot{E}_{P,HTC\ tv}$
Overall system	$\dot{E}_{F,tot} = \dot{W}_{HTC} + \dot{W}_{LTC}$ $\dot{E}_{L,tot} = \dot{E}_{P,cond}$	$\dot{E}_{P,tot} = \dot{E}_{P,ev}$	$\dot{E}_{D,tot} = \sum \dot{E}_{D,k}$

Division of exergy destruction by the overall fuel exergy associated with the system, on the whole, is calculated by Eq. (8).

$$y_k = \frac{\dot{E}_{D,k}}{\dot{E}_{F,tot}} \quad (8)$$

The exergy destruction proportion in the  $k^{th}$  components in the overall exergy destruction is found by Eq. (9).

$$y_k^* = \frac{\dot{E}_{D,k}}{\dot{E}_{D,tot}} \quad (9)$$

## ADVANCED EXERGY ANALYSIS

Even though conventional exergy analysis is a productive approach in pinpointing the causes, locations, and magnitudes of particular types of irreversibility [63], key limitations include the inability to identify confounding effects (e.g., the impact of interactions between components in a system), the failure to identify root causes of exergy destructions that take place in equipment, and the absence of improvement possibilities for equipment. In complex systems, particularly those containing multiple interacting elements, these interactions must often be considered to facilitate system optimisation under conventional exergy analysis [36]. Contrastingly, advanced exergy analysis accounts for these limitations, thus illuminating thermodynamic systems from a novel vantage point. This procedure splits exergy destruction into multiple parts, comprising avoidable-unavoidable and endogenous-exogenous exergy destructions. Designers can determine how

to improve an overall system relying on combining these parts, and advanced exergy analysis offers a more robust foundation for exergo-environmental and exergo-economic investigations [48].

It is possible to introduce specific enhancements to safeguard against structural modifications from a component of the exergy destruction of a system or the components' efficiency. The exergy destruction can be avoided via either operational enhancements or technical designs (or a combination of the two). It is regarded as an avoidable part of the exergy destruction ( $\dot{E}_{D,k}^{AV}$ ). The amount of  $\dot{E}_{D,k}^{AV}$  for the  $k^{th}$  the component plays a significant role in determining the improvement steps and predicting the improvement potential of a system. The exergy destruction associated with physical, economic and technological constraints is considered as an unavoidable part of the exergy destruction of the  $k^{th}$  component ( $\dot{E}_{D,k}^{UN}$ ), even if the best technology is applied. Thus, the exergy destruction can be split into avoidable and unavoidable parts, as seen in Eq. (10) [18,39,64].

$$\dot{E}_{D,k}^{RL} = \dot{E}_{D,k}^{UN} + \dot{E}_{D,k}^{AV} \quad (10)$$

The formation of the exergy destruction caused by the component itself is called endogenous part of the exergy destruction ( $\dot{E}_{D,k}^{EN}$ ), whereas exogenous part of the exergy destruction is the exergy destruction that results from the relationship of the examined component with the other components ( $\dot{E}_{D,k}^{EX}$ ). Total of  $\dot{E}_{D,k}^{EN}$  and  $\dot{E}_{D,k}^{EX}$  gives the exergy destruction of the real process, as indicated in Eq. (11) [18,19,36,39,65].

$$\dot{E}_{D,k}^{RL} = \dot{E}_{D,k}^{EN} + \dot{E}_{D,k}^{EX} \quad (11)$$

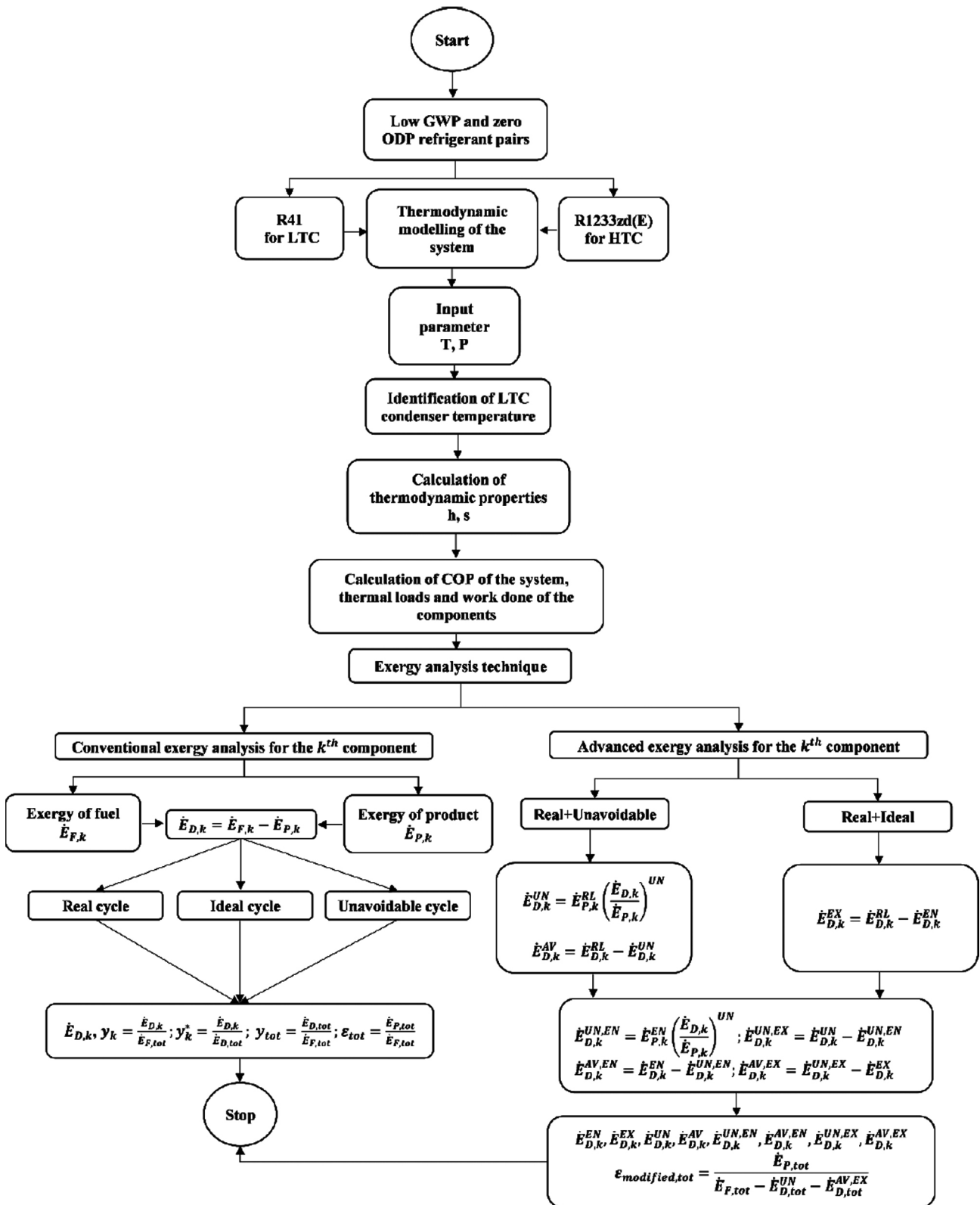


Figure 2. Flow chart for solution procedure.

Technological and economic limitations determine the minimum value of the exergy destruction. The unavoidable part of the exergy destruction of the  $k^{th}$  component is calculated by considering each component separated from the system. The exergy destruction rate per unit product exergy ( $\dot{E}_D/\dot{E}_P$ ) <sub>$k$</sub> <sup>UN</sup> is calculated by assuming that the component of a system operates under high efficiency and low losses. The unavoidable part of the exergy destruction of the  $k^{th}$  component can be explained in Eq. (12), including the product exergy rate of the real process [18,19,36,39].

$$\dot{E}_{D,k}^{UN} = \dot{E}_{P,k}^{RL} \left( \dot{E}_D / \dot{E}_P \right)_k^{UN} \quad (12)$$

If the unavoidable part of the exergy destruction of the  $k^{th}$  component is well-known, the avoidable part of the exergy destruction is obtained by Eq. (13) [40].

$$\dot{E}_{D,k}^{AV} = \dot{E}_{D,k}^{RL} - \dot{E}_{D,k}^{UN} \quad (13)$$

The unavoidable part of the exergy destruction of the  $k^{th}$  component calculated by the advanced exergy analysis method is split into endogenous and exogenous parts, which are then split into unavoidable-endogenous in Eq. (14), unavoidable-exogenous in Eq. (15), avoidable-endogenous in Eq. (16) and avoidable-exogenous in Eq. (17) of the exergy destruction of the  $k^{th}$  component [16]. The unavoidable-endogenous ( $\dot{E}_{D,k}^{UN,EN}$ ) part of the exergy destruction of the  $k^{th}$  component cannot be reduced due to technical limitations related to the component. In contrast, the unavoidable-exogenous ( $\dot{E}_{D,k}^{UN,EX}$ ) part of the exergy destruction of the  $k^{th}$  component cannot be reduced due to technical limitations in the other components of the overall system for the given structure. The avoidable-endogenous ( $\dot{E}_{D,k}^{AV,EN}$ ) part of the exergy destruction of the  $k^{th}$  component can be reduced by making improvements in the efficiency of the  $k^{th}$  component, and the ( $\dot{E}_{D,k}^{AV,EX}$ ) part of the exergy destruction of the  $k^{th}$  component can be reduced by improving the structure of the overall system, the efficiency of the other components and the efficiency of the  $k^{th}$  component [16, 19, 36, 39-41, 45, 61, 62].

$$\dot{E}_{D,k}^{UN,EN} = \dot{E}_{P,k}^{EN} \left( \dot{E}_D / \dot{E}_P \right)_k^{UN} \quad (14)$$

$$\dot{E}_{D,k}^{UN,EX} = \dot{E}_{D,k}^{UN} - \dot{E}_{D,k}^{UN,EN} \quad (15)$$

$$\dot{E}_{D,k}^{AV,EN} = \dot{E}_{D,k}^{EN} - \dot{E}_{D,k}^{UN,EN} \quad (16)$$

$$\dot{E}_{D,k}^{AV,EX} = \dot{E}_{D,k}^{EX} - \dot{E}_{D,k}^{UN,EX} \quad (17)$$

The modified exergy efficiency of the CRS is designated by Eq. (18) [18, 62].

$$\mathcal{E}_{modified,tot} = \frac{\dot{E}_{P,tot}^{RL}}{\dot{E}_{F,tot}^{RL} - \dot{E}_{D,tot}^{UN} - \dot{E}_{D,tot}^{AV,EX}} \quad (18)$$

In comparison to conventional energy analysis, advanced energy analysis is a more complicated process. This can be facilitated by creating a solution procedure flow chart in Figure 2 to make it possible to follow the CRS analysis, as inspired by Ref. [40].

## SIMULATION RESULTS AND DISCUSSION

In this study, a CRS, a system capable of meeting low-temperature refrigeration requirements with a refrigeration capacity of 1 kW, is used to conduct advanced exergy analysis. Referring to Table 2, R41 in LTC and R1233zd(E) in HTC are selected because both refrigerants cause minimum environmental damage and do not contribute to ozone destruction. Before the advanced exergy analysis approach, energy and exergy-based thermodynamic analyses are conducted to obtain prior knowledge regarding the system investigated. For all the computations, Thermopy library is used in Python programming platform (version 3.7.4).

## MODEL VALIDATION OF THE SIMULATION

The present model of this study is compared with the existing models in the literature. This is carried out to test how accurate the computer code that is developed for simulations of analyses. Figure 3 shows that the analysis results of R170-R161 CRS by Ref. [34] are compared with those of this study under the same working conditions ( $T_{cond} = 40^\circ\text{C}$ ,  $T_{ev} = -40^\circ\text{C}$ ,  $\Delta T = 5^\circ\text{C}$ ). The results show that the COP values found by Ref. [34] and by this study are in good agreement, with a difference of approximately 0.003%. Figure 4 presents that comparison of this study's model with the reference model of Ref. [27] is made in terms of exergy efficiency with varying evaporator temperatures for R41/R404A under the same working conditions ( $T_{ev} = -45^\circ\text{C}$ ,  $T_{cond} = 40^\circ\text{C}$ ,  $\Delta T = 5^\circ\text{C}$ ). The deviation between the two compared models is at a minimum level, a difference of only 0.02%.

## IDENTIFICATION OF AN OPTIMAL LTC CONDENSER TEMPERATURE FOR EACH CYCLE

An optimum LTC condenser temperature is perhaps the most crucial operating parameter. The determination of an optimum LTC condenser temperature under all ideal, real and unavoidable conditions indicates that the CRS can operate at maximum performance. Therefore, Figure

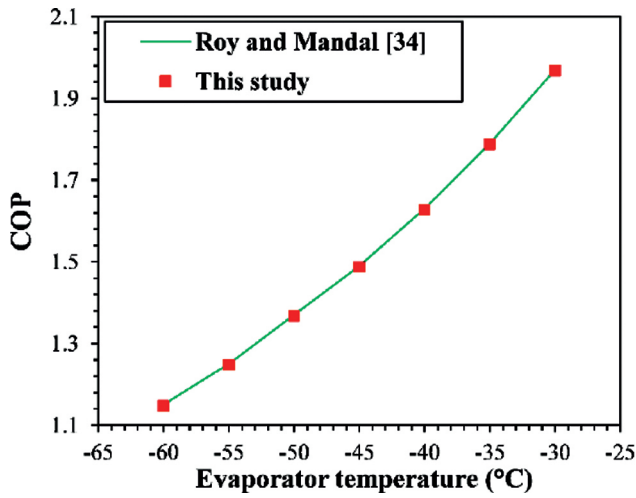


Figure 3. Model validation of the reference model of Roy and Mandal [34].

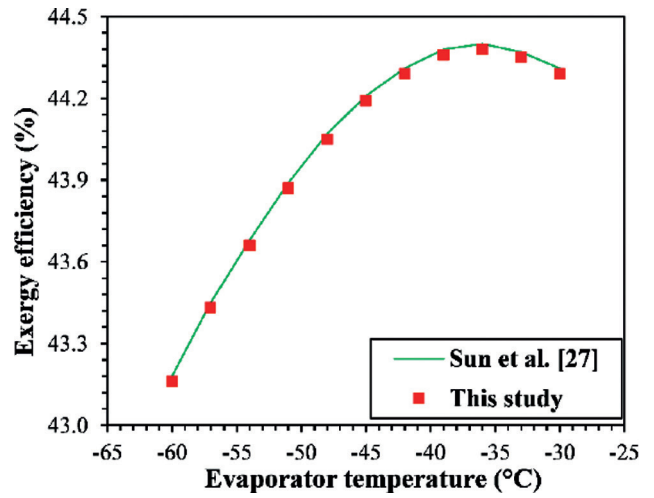


Figure 4. Model validation of the reference model of Sun et al. [27].

Table 7. Thermodynamic properties at each point of the CRS under real operating conditions

Stream	$T$ (°C)	$P$ (kPa)	$h$ (kJ/kg)	$s$ (kJ/kgK)	$\dot{m}$ (kg/s)	$e$ (kJ/kg)	$\dot{E}$ (kW)
1	-60	252.1	523.4	2.606	0.002982	83.6	0.2493
2	96.38	1794	688.6	2.739	0.002982	209	0.6232
3	-4.8	1794	188	0.9565	0.002982	240	0.7155
4	-60	252.1	188	1.032	0.002982	217.5	0.6486
5	-9.8	30.38	397.9	1.752	0.01007	-20.64	-0.2079
6	54.61	215.4	445.8	1.795	0.01007	14.66	0.1477
7	40	215.4	249.7	1.169	0.01007	4.998	0.05035
8	-9.8	30.38	249.7	1.19	0.01007	-1.053	-0.01061
9	25	101.3	104.8	0.3669	0.09448	0	0
10	30	101.3	125.8	0.4365	0.09448	0.1734	0.01639
11	-50	101.3	-429.3	-1.607	0.1165	54.46	6.344
12	-55	101.3	-437.9	-1.646	0.1165	57.48	6.696

5 illustrates the change in COP and exergy efficiency of the CRS, respectively, as a function of LTC condenser temperature ranging from -25 to 15°C. The CRS's technological limitations, the unavoidable operating conditions, causes COP and exergy efficiency to be 1.61 (Figure 5a) and 56.57% (Figure 5b) at an LTC condenser temperature of -12°C, respectively. The efficiency based on the CRS's energy and exergy cannot theoretically exceed COP of 2.165 (Figure 5a) and exergy efficiency of 76.07% (Figure 5b), respectively, at a LTC condenser temperature of -21.8°C. Considering the real conditions as the possible cycle to be applied, COP and exergy efficiency of the CRS at an optimum LTC condenser temperature of 4.8°C are 1.025 (Figure 5a) and 36% (Figure 5b), respectively.

## RESULTS OF THE ENERGY AND CONVENTIONAL EXERGY ANALYSIS

Energy (the first law of thermodynamics) and conventional exergy analyses, which have been widely adopted before applying the advanced exergy approach, are considered first. In this regard, the thermodynamic performance values of the CRS, which operate under ideal, real and unavoidable conditions, are computed based on energy and conventional exergy approaches. Tables 7-9 outlines each stage's thermodynamic properties in the CRS for real, ideal and unavoidable operating conditions, respectively. In the light of the main data required for the CRS specified in Table 4, real, ideal and unavoidable conditions are

calculated. The last two columns in Tables 7-9 depict the exergy values at each CRS point. Advanced exergy analysis is mediated by ideal, real, and unavoidable cycles, so the calculation of exergy destruction in each of these cycles is conducted for all CRS components. The values at points 11 and 12 in Tables 7-9, the overall system exergy of the product ( $\dot{E}_{B,tot} = \dot{E}_{P,ev}$ ) does not fluctuate, so the mass flow rates associated with the secondary working fluid for the evaporator are identical, which can also be derived from the fixed refrigeration capacity, as reported by Ref. [47].

The conventional exergy analysis results for each component are given in Tables 10-12. The exergy destruction

occurring under real, ideal, and unavoidable cycle conditions is calculated for each CRS component. These cycles mentioned above facilitate the performance of the advanced exergy analysis. The conventional exergy analysis results show which component has a more exergy destruction rate. Referring Table 10, the highest exergy destruction rate in the HTC compressor (0.1277 kW or 21%), followed by the LTC compressor (0.1182 kW or 19.52), cascade condenser (0.1050 kW or 17.26%), condenser (0.0810 kW or 13.31%), LTC throttle valve (0.0669 kW or 11%), HTC throttle valve (0.0610 kW or 10.02%) and evaporator (0.0480 kW or 7.88%). Reducing exergy destruction rates is a requirement

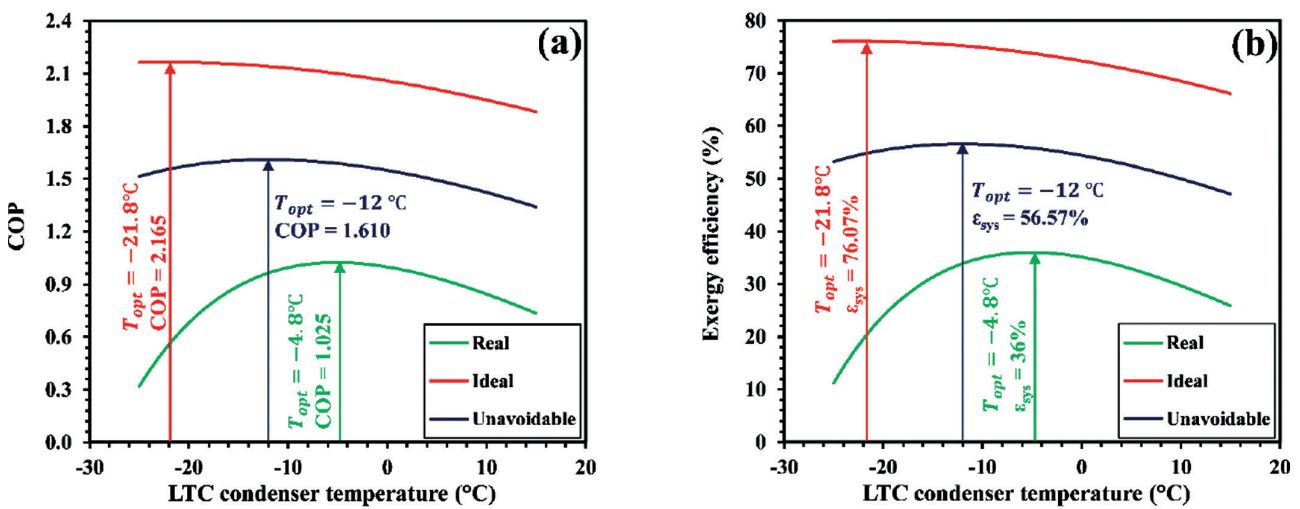


Figure 5. Identification of an optimum LTC condenser temperature for three cycles.

Table 8. Thermodynamic properties at each point of the CRS under ideal operating conditions

Stream	$T$ (°C)	$P$ (kPa)	$h$ (kJ/kg)	$s$ (kJ/kgK)	$\dot{m}$ (kg/s)	$e$ (kJ/kg)	$\dot{E}$ (kW)
1	-55	314	526	2.569	0.002596	97.3	0.2526
2	17.33	1075	594.9	2.569	0.002596	166.2	0.4314
3	-21.8	1075	147	0.8024	0.002596	244.9	0.6358
4	-55	314	140.9	0.8024	0.002596	238.8	0.62
5	-21.8	16.42	389.3	1.757	0.007358	-30.8	-0.2266
6	31.9	154.5	427.8	1.757	0.007358	7.686	0.05655
7	30	154.5	237.1	1.129	0.007358	4.543	0.03343
8	-21.8	16.42	231.2	1.129	0.007358	-1.362	-0.01002
9	25	101.3	104.8	0.3669	0.06706	0	0
10	30	101.3	125.8	0.4365	0.06706	0.1734	0.01163
11	-50	101.3	-429.3	-1.607	0.1165	54.46	6.344
12	-55	101.3	-437.9	-1.646	0.1165	57.48	6.696

<sup>a</sup>The condenser is supposed here to be a productive component. The condensation process heat is released into the environment for each cycle (Tables 10-12), then  $\dot{E}_{L,tot} = \dot{E}_{P,cond}$  (Table 6). However, the condenser is a dissipative component without exergy of product or exergy efficiency. The product value is determined to make it easier to conduct advanced exergy analysis [36].

**Table 9.** Thermodynamic properties at each point of the CRS under unavoidable operating conditions

Stream	$T$ (°C)	$P$ (kPa)	$h$ (kJ/kg)	$s$ (kJ/kgK)	$\dot{m}$ (kg/s)	$e$ (kJ/kg)	$\dot{E}$ (kW)
1	-58	275.6	524.5	2.591	0.002823	89.17	0.2517
2	47.4	1456	627.2	2.608	0.002823	186.8	0.5273
3	-12	1456	170.3	0.8911	0.002823	241.7	0.6822
4	-58	275.6	170.3	0.9436	0.002823	226	0.6381
5	-15	23.48	394.1	1.754	0.008557	-24.93	-0.2133
6	38.74	183	432.8	1.764	0.008557	10.88	0.09311
7	35	183	243.4	1.149	0.008557	4.719	0.04038
8	-15	23.48	243.4	1.17	0.008557	-1.563	-0.01337
9	25	101.3	104.8	0.3669	0.07751	0	0
10	30	101.3	125.8	0.4365	0.07751	0.1734	0.01344
11	-50	101.3	-429.3	-1.607	0.1165	54.46	6.344
12	-55	101.3	-437.9	-1.646	0.1165	57.48	6.696

**Table 10.** Results obtained from conventional exergy analysis under real cycle conditions

Components	$\dot{E}_{E,k}^{RL}$ (kW)	$\dot{E}_{P,k}^{RL}$ (kW)	$\dot{E}_{D,k}^{RL}$ (kW)	$\dot{E}_L^{RL}$ (kW)	$y_k$ (%)	$y_k^*$ (%)
LTC throttle valve	0.7155	0.6486	0.0669	-	6.858	11
HTC throttle valve	0.05035	-0.0106	0.0610	-	6.245	10.02
LTC compressor	0.4927	0.3739	0.1182	-	12.16	19.52
HTC compressor	0.4834	0.3556	0.1277	-	13.09	21
Cascade condenser	0.8311	0.7261	0.1050	-	10.75	17.26
Evaporator	0.3993	0.3514	0.0480	-	4.913	7.884
Condenser <sup>a</sup>	0.09737	0.0164	0.0810	-	8.298	13.31
Overall system	0.9761	0.3514	0.6083	0.0164	62.314	100

**Table 11.** Results obtained from conventional exergy analysis under ideal cycle conditions

Components	$\dot{E}_{E,k}^{TH}$ (kW)	$\dot{E}_{P,k}^{TH}$ (kW)	$\dot{E}_{D,k}^{TH}$ (kW)	$\dot{E}_L^{TH}$ (kW)	$y_k$ (%)	$y_k^*$ (%)
LTC throttle valve	0.6358	0.6200	0.0158	-	3.422	15.98
HTC throttle valve	0.03343	-0.0100	0.0435	-	9.407	43.92
LTC compressor	0.1788	0.1788	0.0000	-	0	0
HTC compressor	0.2831	0.2831	0.0000	-	0	0
Cascade condenser	0.658	0.6458	0.0122	-	2.643	12.34
Evaporator	0.3674	0.3514	0.0160	-	3.458	16.14
Condenser <sup>a</sup>	0.02313	0.0116	0.0115	-	2.488	11.62
Overall system	0.4619	0.3514	0.0989	0.0116	21.418	100

**Table 12.** Results obtained from conventional exergy analysis under unavoidable cycle conditions

Components	$\dot{E}_{Fk}^{UN}$ (kW)	$\dot{E}_{Bk}^{UN}$ (kW)	$\dot{E}_{D,k}^{UN}$ (kW)	$\dot{E}_L^{UN}$ (kW)	$y_k$ (%)	$y_k^*$ (%)
LTC throttle valve	0.6822	0.6381	0.0442	–	7.11	17.23
HTC throttle valve	0.04038	–0.0134	0.0538	–	8.654	20.97
LTC compressor	0.29	0.2756	0.0143	–	2.308	5.592
HTC compressor	0.3312	0.3064	0.0248	–	3.997	9.685
Cascade condenser	0.7406	0.6956	0.0450	–	7.247	17.56
Evaporator	0.3864	0.3514	0.0350	–	5.632	13.65
Condenser <sup>a</sup>	0.05272	0.0134	0.0393	–	6.323	15.32
Overall system	0.6212	0.3514	0.2564	0.0134	41.271	100

to boost the performance of the CRS. However, it is impossible to determine whether irreversibilities originate from other components or the components themselves because conventional exergy destruction cannot give us an idea of what these irreversibilities cause. The reason is that elimination of these restrictive factors can only be achieved through an advanced exergy approach.

## RESULTS OF THE ADVANCED EXERGY ANALYSIS

Table 13 and Figures 6-12 outline the results of the real exergy destruction ( $\dot{E}_{D,k}^{RL}$ ) split into various parts ( $\dot{E}_{D,k}^{EN}$ ,  $\dot{E}_{D,k}^{EX}$ ,  $\dot{E}_{D,k}^{UN}$ ,  $\dot{E}_{D,k}^{AV}$ ,  $\dot{E}_{D,k}^{AV,EN}$ ,  $\dot{E}_{D,k}^{AV,EX}$ ,  $\dot{E}_{D,k}^{UN,EN}$ ,  $\dot{E}_{D,k}^{UN,EX}$ ) for advanced exergy analysis. Information can be obtained about how much of the exergy destruction that occurs from the component's internal irreversibility and/or the component's interaction as the external irreversibility can be avoided or unavaid. As can be seen from both Table 13 and Figures 6-12, the  $\dot{E}_{D,k}^{EN}$  of the evaporator (0.0480 kW or 100%), HTC throttle valve (0.0536 kW or 88%), and condenser (0.0574 kW or 70.82%) and cascade condenser (0.0538 kW or 51.26%) is greater than the  $\dot{E}_{D,k}^{EX}$  of the other components of the CRS ( $\dot{E}_{D,k}^{EN} > \dot{E}_{D,k}^{EX}$ ). All of the evaporator's exergy destruction takes place in the endogenous part so that the irreversibility for this component only results from the component itself; therefore, there is no exergy destruction in the exogenous part of this component. It should be pointed out that in Table 13 that  $\dot{E}_{D,k}^{EX}$  of the LTC compressor (0.09 kW or 75.81%), LTC throttle valve (0.045 kW or 67.19%) and HTC compressor (0.0843 kW or 66.02%) are much greater than the  $\dot{E}_{D,k}^{EN}$ , so the exergy destruction of these components is dependent to a great extent on other components of the CRS, which means that improvements in the other system components can reduce the  $\dot{E}_{D,k}^{EX}$  of the mentioned components, increasing the efficiency of the CRS.

It is worth noting from both Table 13 and Figures 6-12 that the  $\dot{E}_{D,k}^{AV}$  of LTC compressor (0.0992 kW or 83.61%),

HTC compressor (0.0989 kW or 77.43%) and cascade condenser (0.0580 kW or 55.24%) are more than the  $\dot{E}_{D,k}^{UN}$ . The other components of the CRS such as condenser (0.0479 kW or 59.15%), LTC throttle valve (0.0449 kW or 67.08%), HTC throttle valve (0.0427 kW or 70%) and evaporator (0.0350 kW or 72.97%) also have the  $\dot{E}_{D,k}^{AV}$ . Still, they remain inferior to the  $\dot{E}_{D,k}^{UN}$ , meaning that the improvement potential for the components mentioned above is quite weak because of the ( $\dot{E}_{D,k}^{UN} > \dot{E}_{D,k}^{AV}$ ). It can be deduced from Table 13 and Figures 6-12 that the efficiencies of these mentioned components ( $\dot{E}_{D,k}^{UN} > \dot{E}_{D,k}^{AV}$  or  $\dot{E}_{D,k}^{UN} < \dot{E}_{D,k}^{AV}$ ) can be improved. There are several ways for increasing efficiency, such as the adoption of technical modifications (e.g. better lubrication system) and advanced technologies or component substitution with components of greater efficiency. Hence, from the perspective of efficiency enhancement, the CRS is highly promising. The exergy destruction rate of the CRS components can be decreased at most by 0.3425 kW or 56.3% of the real part of exergy destruction within conventional exergy analysis.

$\dot{E}_{D,k}^{AV,EN}$  and  $\dot{E}_{D,k}^{AV,EX}$  are highly informative about cycle optimisation, so it is necessary to determine  $\dot{E}_{D,k}^{AV,EN}$ ,  $\dot{E}_{D,k}^{AV,EX}$ ,  $\dot{E}_{D,k}^{UN,EN}$  and  $\dot{E}_{D,k}^{UN,EX}$ . Nevertheless,  $\dot{E}_{D,k}^{AV,EN}$  should be prioritised, followed by a decrease in  $\dot{E}_{D,k}^{AV,EX}$ . Therefore, in the context of cycle enhancement initiatives, alteration of components with higher  $\dot{E}_{D,k}^{AV,EN}$  should be prioritised. By making the  $k^{th}$  component more efficient and enhancing its working condition, decrease in the associated  $\dot{E}_{D,k}^{AV,EN}$  can be achieved. Improving the cycle structure and making related CRS components more efficient are the two approaches for decreasing  $\dot{E}_{D,k}^{AV,EX}$  [61]. It can be inferred from Table 13 and Figures 6-12 that the  $\dot{E}_{D,k}^{AV,EN}$  of the cascade condenser (0.0297 kW or 28.32%), condenser (0.0234 kW or 28.93%), HTC throttle valve (0.0161 kW or 26.36%) and evaporator (0.0130 kW or 27.03%) are higher than the  $\dot{E}_{D,k}^{AV,EX}$ . Hence, these components with the high  $\dot{E}_{D,k}^{AV,EN}$  should be given priority because technical modifications to these components can enhance their efficiency and the efficiency of the CRS.

**Table 13.** Results obtained from advanced exergy analysis for the various parts of the exergy destruction

Components	$\dot{E}_{D,k}^{RL}$	$\dot{E}_{D,k}^{EN}$	$\dot{E}_{D,k}^{EX}$	$\dot{E}_{D,k}^{UN}$	$\dot{E}_{D,k}^{AV}$	$\dot{E}_{D,k}^{AV}$ (kW)		$\dot{E}_{D,k}^{UN}$ (kW)	
	(kW)	(kW)	(kW)	(kW)	(kW)	$\dot{E}_{D,k}^{AV,EN}$	$\dot{E}_{D,k}^{AV,EX}$	$\dot{E}_{D,k}^{UN,EN}$	$\dot{E}_{D,k}^{UN,EX}$
						(kW)	(kW)	(kW)	(kW)
LTC throttle valve	0.0669	0.0220	0.0450	0.0449	0.0220	0.0072	0.0148	0.0147	0.0302
HTC throttle valve	0.0610	0.0536	0.0074	0.0427	0.0183	0.0161	0.0022	0.0375	0.0052
LTC compressor	0.1187	0.0287	0.0900	0.0195	0.0992	0.0240	0.0752	0.0047	0.0147
HTC compressor	0.1277	0.0434	0.0843	0.0288	0.0989	0.0336	0.0653	0.0098	0.0190
Cascade condenser	0.1050	0.0538	0.0512	0.0470	0.0580	0.0297	0.0283	0.0241	0.0229
Evaporator	0.0480	0.0480	0.0000	0.0350	0.0130	0.0130	0.0000	0.0350	0.0000
Condenser	0.0810	0.0574	0.0236	0.0479	0.0331	0.0234	0.0097	0.0339	0.0140
Overall system	0.6082	0.3067	0.3015	0.2657	0.3425	0.1470	0.1955	0.1597	0.1060
$\epsilon_{modified,tot}$	68%								

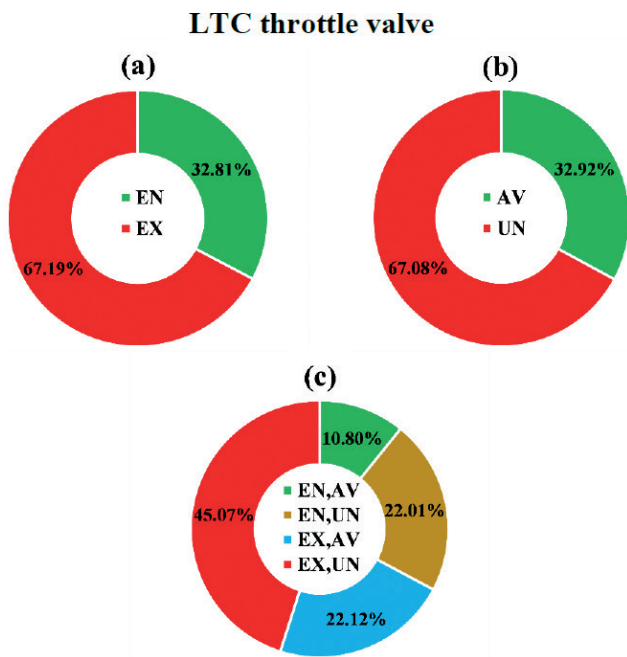


**Figure 6.** The distribution of the exergy destruction of LTC throttle valve. Representation of (a) EN,EX (b) AV,UN (c) EN,AV / EN,UN / EX,AV / EX,UN.

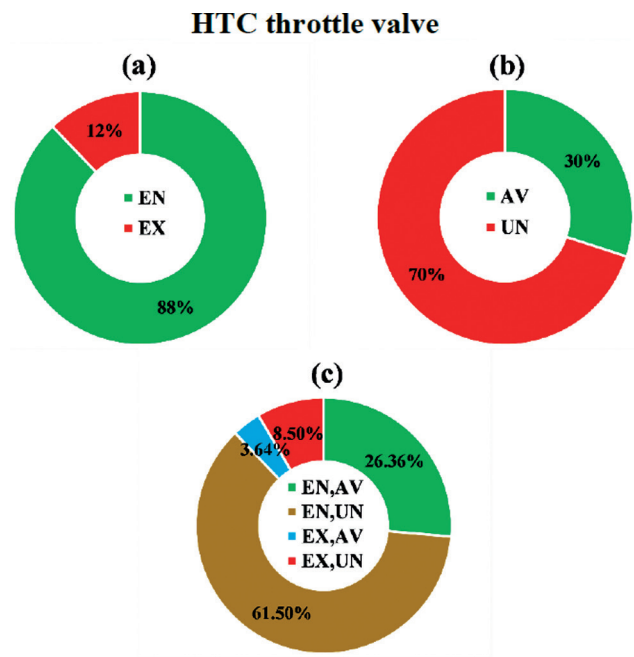


**Figure 7.** The distribution of the exergy destruction of HTC throttle valve. Representation of (a) EN,EX (b) AV,UN (c) EN,AV / EN,UN / EX,AV / EX,UN.

Looking again at Table 13 and Figures 6-12, the fact that the LTC compressor (0.0752 kW or 63.39%) and HTC compressor (0.0653 kW or 51.12%) have the highest  $\dot{E}_{D,k}^{AV,EX}$  and a change in the efficiency of the other components of the CRS will have a significant influence on improving the performance of these components. The  $\dot{E}_{D,k}^{AV,EX}$  of the cascade condenser (0.0283 kW or 26.93%), condenser (0.0097 kW or 11.90%), HTC throttle valve (0.0022 kW or 5.10%) and evaporator (0 kW or 0%) is less than the  $\dot{E}_{D,k}^{UN,EN}$ ; for this

reason, optimising the efficiency of these components will play a central role in boosting the CRS performance. It is also observed from Table 13 and Figures 6-12 that  $\dot{E}_D^{AV,EN}$  (0.1470 kW or 24.17%) of the CRS partially lower than the  $\dot{E}_D^{UN,EN}$  (0.1597 kW or 26.26%) of the CRS due to the high  $\dot{E}_{D,k}^{UN,EN}$  of HTC throttle valve (0.0375 kW or 61.50%), condenser (0.0339 kW or 41.89%) and evaporator (0.035 kW or 72.97%). The  $\dot{E}_{D,k}^{AV,EX}$  of the LTC compressor (0.0752 kW or 63.39%), HTC compressor (0.0653 kW or 51.12%) and

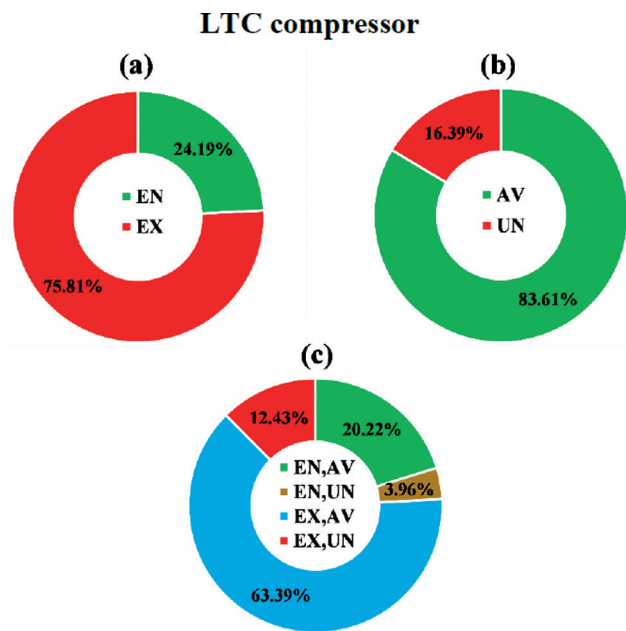


Figure 8. The distribution of the exergy destruction of LTC compressor. Representation of (a) EN,EX (b) AV,UN (c) EN,AV / EN,UN / EX,AV / EX,UN.

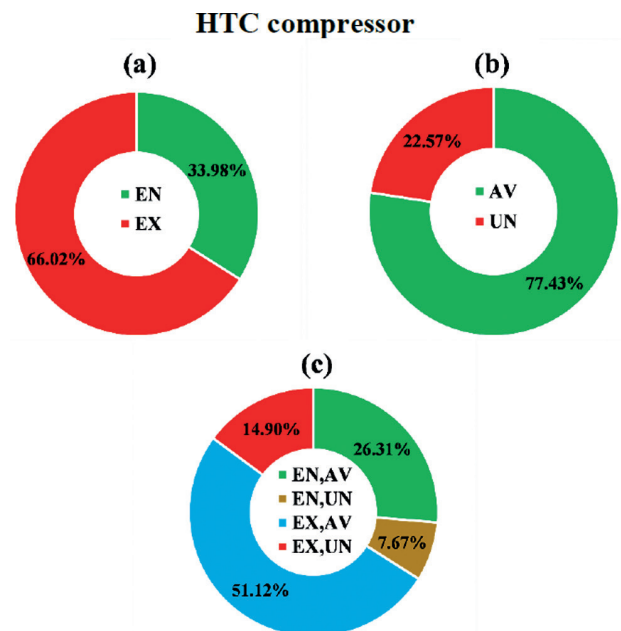


Figure 9. The distribution of the exergy destruction of HTC compressor. Representation of (a) EN,EX (b) AV,UN (c) EN,AV / EN,UN / EX,AV / EX,UN.

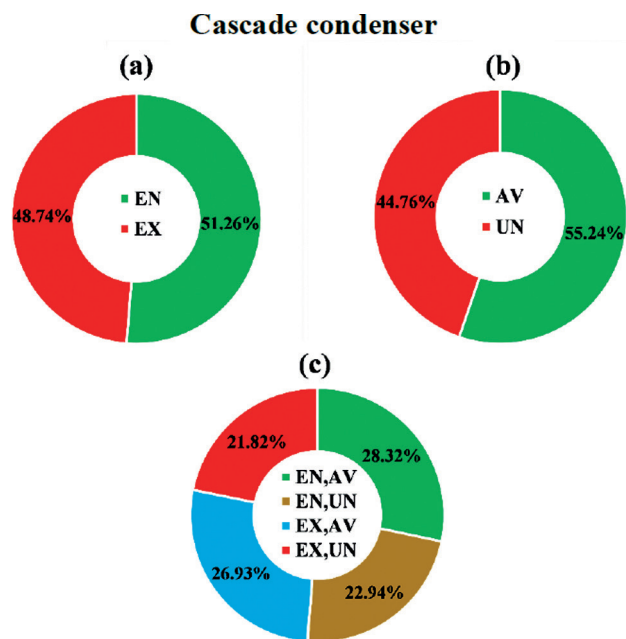


Figure 10. The distribution of the exergy destruction of cascade condenser. Representation of (a) EN,EX (b) AV,UN (c) EN,AV / EN,UN / EX,AV / EX,UN.

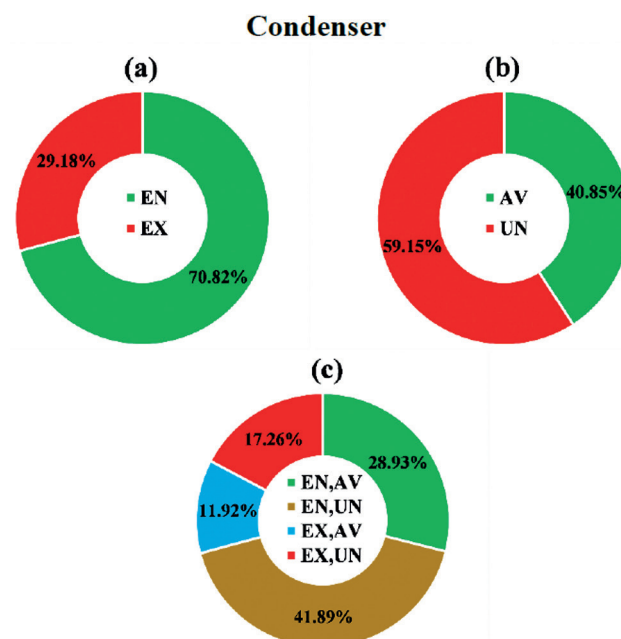
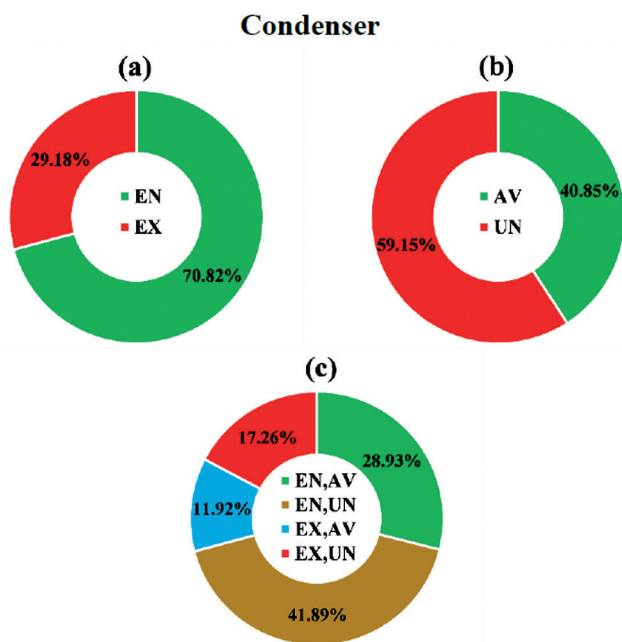


Figure 11. The distribution of the exergy destruction of evaporator. Representation of (a) EN,EX (b) AV,UN (c) EN,AV / EN,UN / EX,AV / EX,UN.

cascade condenser (0.0283 kW or 26.93%) is higher than the  $\dot{E}_{D,k}^{UN,EX}$ ; thus, an improvement in component efficiency leads to a reduction in the  $\dot{E}_{D,k}^{AV,EX}$  of the other components of the CRS. The value specified in the bottom line of Table

13 is the modified exergy efficiency calculated by Eq. (22). Consequently, the exergy efficiency of the CRS leaps from 36 to 68% with necessary improvements required to the components of the CRS.



**Figure 12.** The distribution of the exergy destruction of condenser. Representation of (a) EN,EX (b) AV,UN (c) EN,AV / EN,UN / EX,AV / EX,UN.

## CONCLUSION

Conventional exergy analysis can quantitatively identify inefficiencies in an energy system. Although it is a newer approach, advanced exergy analysis can specify the origins of irreversibilities and real improvement potential. In this paper, an advanced exergy approach is applied in conjunction with a conventional exergy analysis to examine the exergy performance of the R41/R1233zd(E) CRS analysed in line with an optimum LTC condenser temperature. The far-reaching implications obtained are listed as follows:

1. The most critical CRS components in the conventional exergy analysis are the HTC compressor, followed by the LTC compressor and cascade condenser, suggesting that the three components should be given the highest priority in optimising the CRS performance. Conversely, the advanced exergy analysis suggests that LTC compressor, HTC compressor, and cascade condenser prioritise improvement due to their high avoidable exergy destruction rates.
2. The CRS's total exergy destruction accounts for the endogenous part of 50.43% and the exogenous part of 49.57%, meaning that interactions between the CRS components remain somewhat lower.
3. The cascade condenser ( $\dot{E}_{D,k}^{EX}$  of 48.74% and  $\dot{E}_{D,k}^{EN}$  of 51.26%) are strongly influenced by both their

structural and interactions of the rest components of the CRS.

4. The LTC compressor is the most dependent on other components of the CRS since it is the component with the most significant exogenous part of the exergy destruction (0.09 kW or 75.82%).
5. The avoidable part of the total exergy destruction is 56.31%, which is slightly more significant than the unavoidable part, meaning that component improvements have high potential to improve the CRS performance.
6. The maximum improvement potentials of LTC compressor and HTC compressor are more significant compared to other components of the CRS because their avoidable exergy destruction rates are 0.0992 kW (83.57%) and 0.0989 kW (77.45%). In contrast, their endogenous-avoidable exergy destruction rates are 0.0240 kW (20.22%) and 0.0336 kW (26.31%), respectively.
7. The HTC throttle valve's inefficiencies, condenser and evaporator are mainly stemmed from the components themselves (internal irreversibility), thereby possessing the high endogenous exergy destruction.
8. The exergy efficiency of the CRS, which is calculated in the conventional exergy analysis, remains at only 36%, while the improvements required for the components soar the exergy efficiency of the CRS to approximately 68%.
9. Advanced exergy approach exhibits a more robust foundation than the conventional exergy approach for exergo-environmental and exergo-economic investigations; therefore, it is vital to make such investigations for the future studies using the refrigerants that harm the least environment.

## NOMENCLATURE

$\dot{E}$	Exergy destruction rate, kW
$\dot{Q}$	Heating or cooling capacity, kW
$\dot{W}$	Work, kW
$\dot{m}$	Mass flow rate, kg/s
$h$	Specific enthalpy, kJ/kg
$P$	Pressure, kPa
$T$	Temperature, °C
$e$	Specific exergy, kJ/kg
$s$	Specific entropy, kJ/(kgK)

### Acronyms

CFC	Chlorofluorocarbon
COP	Coefficient of performance
CRS	Cascade refrigeration system
GWP	Global warming potential
HCFC	Hydrochlorofluorocarbon
HFC	Hydrofluorocarbon

HFO	Hydrofluoro-olefin
HTC	High temperature circuit
LTC	Low temperature circuit
NBP	Normal boiling point, °C
ODP	Ozone depletion potential
VCRS	Vapor compression refrigeration system

## Subscript

0	Thermodynamic dead state
1, 2, 3, ..	State points
CHX	Cascade heat exchanger or cascade condenser
cond	Condenser
D	Destruction
ev	Evaporator
F	Fuel
i	Isentropic
in	Inlet
k	k-th component
L	Loss
out	Outlet
P	Product
tot	Total
tv	Throttle valve
w	Water

## Superscripts

AV	Avoidable
AV, EN	Avoidable-Endogenous
AV, EX	Avoidable-Exogenous
CH	Chemical
EN	Endogenous
EX	Exogenous
KE	Kinetic exergy
PE	Potential exergy
PH	Physical
R	Real
TH	Theoretical
UN	Unavoidable
UN,EN	Unavoidable-Endogenous
UN,EX	Unavoidable-Exogenous

## Greek symbols

$\Delta T$	Temperature difference
$\eta$	Efficiency of compressor
$\gamma$	Exergy destruction ratio
$\varepsilon$	Exergy efficiency

## ACKNOWLEDGEMENT

Caner Aktemur is a PhD scholarship holder from the Council of Higher Education (YÖK) in the field of Renewable Energy and Energy Storage, which is one of the 100 national priority areas determined by YÖK within the scope of the 100/2000 Program.

## AUTHORSHIP CONTRIBUTIONS

Authors equally contributed to this work.

## DATA AVAILABILITY STATEMENT

The authors confirm that the data that supports the findings of this study are available within the article. Raw data that support the finding of this study are available from the corresponding author, upon reasonable request.

## CONFLICT OF INTEREST

The author declared no potential conflicts of interest with respect to the research, authorship, and/or publication of this article.

## ETHICS

There are no ethical issues with the publication of this manuscript.

## REFERENCES

- [1] Yataganbaba A, Kilicarlan A, Kurtbas I. Exergy analysis of R1234yf and R1234ze as R134a replacements in a two evaporator vapour compression refrigeration system. *Int J Refrig* 2015;60:26–37. [\[CrossRef\]](#)
- [2] Polzot A, Dipasquale C, D'Agaro P, Cortella G. Energy benefit assessment of a water loop heat pump system integrated with a CO2 commercial refrigeration unit. *Energy Proced* 2017;123:36–45.
- [3] Miyara A, Onaka Y, Koyama S. Ways of next generation refrigerants and heat pump/refrigeration systems. *Int J Air Conditioning Refrig* 2012;20:1–11. [\[CrossRef\]](#)
- [4] Montzka SA, Dutton GS, Yu P, Ray E, Portmann RW, Daniel JS, et al. An unexpected and persistent increase in global emissions of ozone-depleting CFC-11. *Nature* 2018;557:413–417. [\[CrossRef\]](#)
- [5] Bolaji BO, Huan Z. Ozone depletion and global warming: Case for the use of natural refrigerant—a review. *Renew Sustain Energy Rev* 2013;18:49–54. [\[CrossRef\]](#)
- [6] Benhadid-Dib S, Benzaoui A. Refrigerants and their environmental impact Substitution of hydro chloro-fluorocarbon HCFC and HFC hydro fluorocarbon. Search for an adequate refrigerant. *Energy Proced* 2012;18:807–816. [\[CrossRef\]](#)
- [7] Persson L, Persson Å, Nilsson M. Multilateral environmental agreements on the ground: lessons from supporting implementation of the Montreal Protocol. *Stockholm Env Inst* 2007. [\[CrossRef\]](#)
- [8] Longo GA, Mancin S, Righetti G, Zilio C, Brown S. Assessment of the low-GWP refrigerants R600a,

- R1234ze(Z) and R1233zd(E) for heat pump and organic Rankine cycle applications. *Appl Therm Eng* 2020;167:114804. [CrossRef]
- [9] Mota-Babiloni A, Navarro-Esbri J, Barragán-Cervera Á, Molés F, Peris B. Analysis based on EU Regulation No 517/2014 of new HFC/HFO mixtures as alternatives of high GWP refrigerants in refrigeration and HVAC systems. *Int J Refrig* 2015;52:21–31. [CrossRef]
- [10] Gupta S, Karanam NK, Konijeti R, Dasore A. Thermodynamic Analysis and Effects of Replacing HFC by Fourth-Generation Refrigerants in VCR Systems. *Int J Air Conditioning Refrig* 2018;26:1–12. [CrossRef]
- [11] Dikmen E, Sahin AS, Deveci OI, Akdag E. Comparative performance analysis of cascade refrigeration system using low GWP refrigerants. *El-Cezeri J Sci Eng* 2020;7:338–345.
- [12] Sun Z, Wang Q, Xie Z, Liu S, Su D, Cui Q. Energy and exergy analysis of low GWP refrigerants in cascade refrigeration system. *Energy* 2019;170:1170–1180. [CrossRef]
- [13] Bellos E, Tzivanidis C. A theoretical comparative study of CO<sub>2</sub> cascade refrigeration systems. *Appl Sci* 2019;9:790. [CrossRef]
- [14] Yilmaz F, Selbas R. Comparative thermodynamic performance analysis of a cascade system for cooling and heating applications. *Int J Green Energy* 2019;16:674–686. [CrossRef]
- [15] Kovaci, T. Energy performance assessment of CO<sub>2</sub> cascade refrigeration systems. *J Appl Sci* 2020;4:22–32.
- [16] Kelly S, Tsatsaronis G, Morosuk T. Advanced exergetic analysis: approaches for splitting the exergy destruction into endogenous and exogenous parts. *Energy* 2009;34:384–391. [CrossRef]
- [17] Fallah M, Mahmoudi SMS, Yari M, Ghiasi RA. Advanced exergy analysis of the Kalina cycle applied for low temperature enhanced geothermal system. *Energy Convers Manag* 2016;108:190–201. [CrossRef]
- [18] Ustaoglu A. Parametric study of absorption refrigeration with vapor compression refrigeration cycle using wet, isentropic and azeotropic working fluids: Conventional and advanced exergy approach. *Energy* 2020;201:117491. [CrossRef]
- [19] Morosuk T, Tsatsaronis G, Schult M. Conventional and advanced exergetic analyses: theory and application. *Arab J Sci Eng* 2013;38:395–404. [CrossRef]
- [20] Morosuk T, Tsatsaronis G. Advanced exergetic evaluation of refrigeration machines using different working fluids. *Energy* 2009;34:2248–2258. [CrossRef]
- [21] Ranendra R, Mandal BK. Exergy analysis of cascade refrigeration system working with refrigerant pairs R41-R404A and R41-R161. *Int Conf Mech Mater Renew Energy* 2017 Dec 8–10; 377: Sikkim, India.,1–6. [CrossRef]
- [22] Dopazo JA, Fernández-Seara J. Experimental evaluation of a cascade refrigeration system prototype with CO<sub>2</sub> and NH<sub>3</sub> for freezing process applications. *Int J Refrig* 2011;34:257–267. [CrossRef]
- [23] Sanz-Kock C, Llopis R, Sánchez D, Cabello R, Torrella E. Experimental evaluation of a R134a/CO<sub>2</sub> cascade refrigeration plant. *Appl Therm Eng* 2014;73:41–50. [CrossRef]
- [24] Shakya A, Faisal N, Chauhan T. Performance analysis of vapour compression cascade refrigeration system using refrigerants R404A and R134a. *Int J Sci Dev Res* 2019;4:319–325.
- [25] Bhattacharyya S, Garai A, Sarkar J. Thermodynamic analysis and optimisation of a novel N<sub>2</sub>O–CO<sub>2</sub> cascade system for refrigeration and heating. *Int J Refrig* 2009;32:1077–1084. [CrossRef]
- [26] Yilmaz F, Selbas R. Energy and exergy analyses of CO<sub>2</sub>/HFE7000 cascade cooling system. *Nat Appl Sci* 2017;21:854–860. [CrossRef]
- [27] Sun Z, Liang Y, Liu S, Ji W, Zang R, Liang R, et al. Comparative analysis of thermodynamic performance of a cascade refrigeration system for refrigerant couples R41/R404A and R23/R404A. *Appl Energy* 2016;184:19–25. [CrossRef]
- [28] Parekh AD, Tailor PR, Patel T. Numerical simulation of R410a-R23 and R404A-R508B cascade refrigeration system. *Int J Mech Aerosp Ind Mechatro Manuf Eng* 2011;5:2063–2067.
- [29] Park H, Kim DH, Kim MS. Thermodynamic analysis of optimal intermediate temperatures in R134a- R410A cascade refrigeration systems and its experimental verification. *Appl Therm Eng* 2013;54:319–327. [CrossRef]
- [30] Cabello R, Sánchez D, Llopis R, Catalán J, Torrella E. Energy evaluation of R152a as drop in replacement for R134a in cascade refrigeration plants. *Appl Therm Eng* 2016;110:972–984. [CrossRef]
- [31] Sachdeva G, Jain V, Kachhwaha SS. Performance study of cascade refrigeration system using alternative refrigerants. *Int Sch Sci Res Innov* 2014;8:522–528.
- [32] Messineo A, Panno D. Performance evaluation of cascade refrigeration systems using different refrigerants. *Int J Air-Cond Refrig* 2012;20:1–8. [CrossRef]
- [33] Sarkar J, Bhattacharyya S, Lal, A. Selection of suitable natural refrigerants pairs for cascade refrigeration system. *Proc Inst Mech Eng Part A: J Power Energy* 2013;227:612–622. [CrossRef]
- [34] Roy R, Mandal BK. Energetic and exergetic performance comparison of cascade refrigeration system using R170-R161 and R41-R404A as refrigerant pairs. *Heat Mass Transf* 2019;55:723–731. [CrossRef]

- [35] Gholamian E, Hanafizadeh P, Ahmadi, P. Advanced exergy analysis of a carbon dioxide ammonia cascade refrigeration system. *Appl Therm Eng* 2018;137:689–699. [\[CrossRef\]](#)
- [36] Morosuk T, Tsatsaronis G, Zhang C. Conventional thermodynamic and advanced exergetic analysis of a refrigeration machine using a Voorhees' compression process. *Energy Convers Manag* 2012;60:143–151. [\[CrossRef\]](#)
- [37] Yu M, Cui, Wang Y, Liu Z, Zhu Z, Yang S. Advanced exergy and exergoeconomic analysis of cascade absorption refrigeration system driven by low-grade waste heat. *ACS Sustain Chem Eng* 2019;7:16843–16857. [\[CrossRef\]](#)
- [38] Aman J, Henshaw P, Ting DS. Advanced exergy analysis Of LiCl-H<sub>2</sub>O absorption air conditioning system. *Proc Ca Soc Mech Eng Int Cong* 2018 May 27-30:Toronto, Canada, p.1–6. [\[CrossRef\]](#)
- [39] Ustaoglu A, Alptekin M, Akay ME, Selbas, R. Enhanced exergy analysis of a waste heat powered ejector refrigeration system for different working fluids. *Int J Exergy* 2017;24:301–324. [\[CrossRef\]](#)
- [40] Zhao H, Yuan T, Gao J, Wang X, Ya J. Conventional and advanced exergy analysis of parallel and series compression-ejection hybrid refrigeration system for a household refrigerator with R290. *Energy* 2019;166:845–861. [\[CrossRef\]](#)
- [41] Sarkar J, Joshi D. Extended Exergy Analysis Based Comparison of Subcritical and Transcritical Refrigeration Systems. *Int J Air Conditioning Refrig* 2016;24:1650009. [\[CrossRef\]](#)
- [42] Colorado-Garrido D. Advanced Exergy Analysis of a Compression–Absorption Cascade Refrigeration System. *J Energy Resour Technol* 2019;141:1–12. [\[CrossRef\]](#)
- [43] Gong S, Boulama KG. Advanced exergy analysis of an absorption cooling machine: Effects of the difference between the condensation and absorption temperatures. *Int J Refrig* 2015;59:224–234. [\[CrossRef\]](#)
- [44] Gong S, Boulama KG. Parametric study of an absorption refrigeration machine using advanced exergy analysis. *Energy* 2014;76:453–467. [\[CrossRef\]](#)
- [45] Acikkalp E, Hepbasli A, Karakoc H. Advanced exergy analysis of a household refrigerator. 20<sup>nd</sup> Cong Therm Sci Technol 2015 Dec 2–5: Balikesir, Turkey, p.1–6.
- [46] Bai T, Yu J, Yan G. Advanced exergy analyses of an ejector expansion transcritical CO<sub>2</sub> refrigeration system. *Energy Convers Manag* 2016;126:850–861. [\[CrossRef\]](#)
- [47] Chen J, Havtun H, Palm B. Conventional and advanced exergy analysis of an ejector refrigeration system. *Appl Energy* 2015;144:139–151. [\[CrossRef\]](#)
- [48] Tsatsaronis G, Morosuk T. Advanced thermodynamic (exergetic) analysis. *J Phys Conf Ser* 2012;395:1–8. [\[CrossRef\]](#)
- [49] Modi N, Pandya B, Patel J, Mudgal A. Advanced exergetic assessment of a vapor compression cycle with alternative refrigerants. *J Energy Resour Technol* 2019;141:1–9. [\[CrossRef\]](#)
- [50] Gullo P, Elmegaard B, Cortella G. Advanced exergy analysis of a R744 booster refrigeration system with parallel compression. *Energy* 2016;107:562–571. [\[CrossRef\]](#)
- [51] Liu J. Performance improvement potential analysis of a booster-assisted ejector refrigeration system. *IEEE Access* 2019;7:58533–58540. [\[CrossRef\]](#)
- [52] Bai T, Yu J, Yan G. Advanced exergy analysis on a modified auto-cascade freezer cycle with an ejector. *Energy* 2016;113:385–398. [\[CrossRef\]](#)
- [53] Duarte-Garza HA, Magee JW. Subatmospheric vapor pressures for fluoromethane (R41), 1, 1-difluoroethane (R152a), and 1, 1, 1-trifluoroethane (R143a) evaluated from internal-energy measurements. *Int J Thermophys* 1999;20:1467–1481.
- [54] Mondéjar ME, McLinden MO, Lemmon EW. Thermodynamic properties of trans-1-chloro-3, 3, 3-trifluoropropene (R1233zd (E)): Vapor pressure (p, ρ, T) behavior, and speed of sound measurements, and equation of state. *J Chem Eng Data* 2015;60:2477–2489. [\[CrossRef\]](#)
- [55] Dubey AM, Kumar S, Agrawal GD. Thermodynamic analysis of a transcritical CO<sub>2</sub>/propylene (R744–R1270) cascade system for cooling and heating applications. *Energy Convers Manag* 2014;86:774783. [\[CrossRef\]](#)
- [56] Yang J, Sun Z, Yu B, Chen, J. Experimental comparison and optimisation guidance of R1233zd (E) as a drop-in replacement to R245fa for organic Rankine cycle application. *Appl Therm Eng* 2018;141:10–19. [\[CrossRef\]](#)
- [57] Tolhoek HA, De Groot SR. A discussion of the first law of thermodynamics for open systems. *Physica* 1952;18:780–790. [\[CrossRef\]](#)
- [58] Lee TS, Liu CH, Chen TW. Thermodynamic analysis of optimal condensing temperature of cascade-condenser in CO<sub>2</sub>/NH<sub>3</sub> cascade refrigeration systems. *Int J Refrig* 2006;29:1100–1108. [\[CrossRef\]](#)
- [59] Rosen MA, Bulucea CA. Using exergy to understand and improve the efficiency of electrical power technologies. *Entropy* 2009;11:820–835. [\[CrossRef\]](#)
- [60] Boles M Cengel Y. *An Engineering Approach*. 4th ed. New York: McGraw-Hill Education, 2014.
- [61] Balli O, Hepbasli A. Energetic and exergetic analyses of T56 turboprop engine. *Energy Convers Manage* 2013;73:106–120. [\[CrossRef\]](#)

- 
- [62] Erbay Z, Hepbasli A. Application of conventional and advanced exergy analyses to evaluate the performance of a ground-source heat pump (GSHP) dryer used in food drying. *Energy Convers Manage* 2014;78:499–507. [\[CrossRef\]](#)
- [63] Ustaoglu A. Conventional and advanced exergy analysis of geothermal energy powered reheat organic rankine cycle. *J Sci Technol* 2020;8:783–800.
- [64] Cziesla F, Tsatsaronis G, Gao Z. Avoidable thermodynamic inefficiencies and costs in an externally fired combined cycle power plant. *Energy* 2006;31:1472–1489. [\[CrossRef\]](#)
- [65] Morosuk T, Tsatsaronis G. Advanced exergy-based methods used to understand and improve energy-conversion systems. *Energy* 2019;169:238–246. [\[CrossRef\]](#)